Partial Differential Equations in Applied Mathematics 16 (2025) 101320

Contents lists available at ScienceDirect

Partial Differential Equations in Applied Mathematics

journal homepage: www.elsevier.com/locate/padiff

Intrinsic dynamics of lumps and multi-soliton solutions to the higher dimensional Boussinesq model

M. Belal Hossen [a,*], Md. Towhiduzzaman [a], Mst. Shekha Khatun [b], Harun-Or- Roshid [b], Md. Amanat Ullah [a]

[a] Department of Mathematics, Uttara University, Bangladesh
[b] Department of Mathematics, Sunamgonj Science and Technology University, Bangladesh

ARTICLE INFO

Keywords:
Boussinesq model
Bi-linear formula
Soliton
Lump wave
Breather wave

ABSTRACT

This research investigates diverse wave behaviors of innovative higher dimensional Boussinesq model (BM) based on Hirota bi-linear technique. From this, firstly we derive lump and multiple soliton solutions. The study explores various dynamic behaviors, including interactions involving one up to four solitons. Additionally, the study analyzes breather waves, twofold periodic wave, periodic line lump wave, and the interactions among bell solitons. Other interactions analyze include lump wave with periodic wave, 1-stripe soliton and 2-stripe solitons. Many of these dynamic properties not yet explored in previous research. The trajectories of these solutions are visualized using Maple software, providing deeper insights into the model's dynamical behavior.

1. Introduction

The development of exact solutions and novel structures in nonlinear partial evolution models (NLPEMs) is a crucial area of study in soliton theory. In latest years, researchers have invested their strength to study on solitonic solutions and various types interactions in NLPEMs, employing numerous analytical methods like(G'/G)-expansion technique,[1] Darboux transform,[2] the exp-function procedure,[3,4] the modified Kudryashov technique,[5] Hirota bilinear technique,[6–8] the sub-equation technique,[9,10] the numerical technique,[11] the fractional derivative methods,[12,13] the Fourier spectral method,[14] and the bilinear network technique.[15,16] Among these, Hirota's bilinear technique is particularly effective for obtaining exact solitonic solutions in NLPEMs. Once the bilinear form of an NLPEM is established, it becomes possible to derive rogue, multi-soliton, and breather wave solutions.

In recent decades, scientists have been infatuated by dynamic solutions, particularly rogue-lump solutions, which can manifest in numerous physical contexts like deep ocean waves, plasma, Bose–Einstein condensates, and nonlinear optics.[17,18] Lou et al. explored lump solutions through the variable separation approach,[19] in 2002, while a multifaceted category of lump-type solutions for the KPI equation was recently developed by Ma et al.[20] Further integrable equations with lump solutions include the Ishimori-I,[21] the Davey–Stewartson-II,[22] the Boussinesq,[23] and the BKP model equations.[24]

Lump wave solution is explicit sensible type solutions wholly relied within limited regions in any directions, while lump waves are restricted to tiny regions in most directions, though not all.[25–27] Rogue waves, known for their large, unpredictable, and rapidly occurring nature, pose significant hazards to deep-sea vessels and are often linked to maritime disasters.[28,29] Recently, researchers have extensively investigated soliton, lump, rogue, and hybrid solution collisions in various nonlinear models.[30,31] Inspired by these studies, our aim is to derive complex wave solutions and interactions, including collisions of bell solitons with periodic lump waves, interactions between lump waves and one or two bell solitons, twofold periodic waves, and two pairs of lump waves arranged in a line, for the (3+1)-D BqE.[32] These interactions not yet previously explored in the integrable (3+1)-D BqE.

The dispersion of gravity waves that occur on the water's terrain, specifically the squarely interaction of a slant waves, is well described by the Boussinesq equation in two dimensions. The (2+1)-D Boussinesq model is one of the NLPDEs that may be expressed as

$$u_{tt} - u_{xx} + 3\left(u^2\right)_{xx} - u_{xxxx} - u_{yy} = 0, \tag{1}$$

It is frequently used in fluid mechanics and was initially presented by Allen and Rowlands in 1997 to describe the uniform flow of lengthy, small-amplitude oscillations on the exterior of shallow water in a canal with a fixed width.

In this paper, we explore an advanced higher dimensional Boussinesq

* Corresponding author.
E-mail address: belalshimul14@gmail.com (M.B. Hossen).

https://doi.org/10.1016/j.padiff.2025.101320
Received 29 August 2025; Received in revised form 17 October 2025; Accepted 20 October 2025
Available online 21 October 2025

model (BM)[32]:

$$u_{tt} - u_{xx} + \left(u^2\right)_{xx} - u_{xxxx} + \frac{1}{4}u_{yy} + u_{yt} + u_{xz} = 0. \tag{2}$$

Previous studies have employed various methods to explore solutions to the Boussinesq equation.[33–39] For instance, Xing Lü et al.[33] explored soliton solutions of Vc-Boussinesq model in higher dimensions using Bäcklund transformation and Painlevé analysis. Sachin et al.[34] explored precise analytical solutions and wave structures for extended (3 +1)-D Boussinesq equation through symmetry analysis. By Sardar sub-equation technique, Sulaiman et al.[35] discover some new types wave phenomena of (3+1)-D Boussinesq equation. Liu and Zhu[36] derived multiple rogue wave solutions using a modified symbolic computation approach, while Wazwaz et. al.[37] explored freak upsurge results of the (3+1)-Dimensional gKP-BM. Singh et al.[38] attained bright- and dark-rogue solutions, and Lu et al.[39] applied the HBM to trace lump solutions in shallow water for two-dimensional generalized BqE. Among the previous investigation, interactive and colliding incident are frequently happened naturally. Such interactions of waves are still unexplored for the new higher dimensional BqE. Owing to this fact, we are very interested to explore interactions such as the collisions of bell solitons with periodic lump waves, interactions among lump waves and bell solitons, two lump waves, twofold periodic waves, and two pairs of lump waves arranged in a line for the model.

This paper is organized as: the bi-linear representation to a given model is covered in Section 2. Section 3 focuses on lump surge propagation using positive quadratic functions. Section 4 deliberated the resulting N-soliton solutions and examine various deformed waves and their interactions. Section 5 addresses three types of solitonic interaction. The important and innovation adresses in Section 6. An enlightenment of the conclusion is conversed in Section 7.

2. Bi-linear formation of the Boussinesq model

We now introduce the potential transformation as

$$u = \lambda(t)q_{xx} \tag{3}$$

where $\lambda = \lambda(t)$is a constant. Switching (3) into (2), gives

$$\lambda q_{xxtt} - \lambda q_{xxxx} + (\lambda q_{xx})^2_{xx} - \lambda q_{xxxxxx} + \frac{1}{4}\lambda q_{xxyy} + \lambda q_{xxyt} + \lambda q_{xxxt} = 0 \tag{4}$$

Integrating once (4) w. r. to$x$, and considering the trivial integration constant, yeilds

$$q_{x,2t} - q_{3x} + \lambda(t)\left(q^2_{2x}\right)_x - q_{5x} + \frac{1}{4}q_{x,2y} + q_{x,yt} + q_{2x,z} = 0 \tag{5}$$

Integrating once more w. r. to x, even assuming the trivial integration constant, we arrive at

$$q_{2t} - q_{2x} + \lambda(t)\left(q^2_{2x}\right) - q_{4x} + \frac{1}{4}q_{2y} + q_{y,t} + q_{x,z} = 0 \tag{6}$$

If $\lambda(t) = 3$ is chosen as $q = 2\ln\ f$and by applying the formula from Appendix (A10) in Reference,[40] (6) for q becomes:

$$E(q) = p_{2t}(q) - p_{2x}(q) + 3q^2_{2x} - p_{4x}(q) + \frac{1}{4}p_{2y}(q) + p_{y,t}(q) + p_{x,z}(q) = 0 \tag{7}$$

Based on the results of the P-polynomial provided in[40,41] and applying the formula from Appendix (A10) in Reference,[40] one obtains

$$D_{tt} - D_{xx} - D_{4x} + \frac{1}{4}D_{2y} + D_{yt} + D_{xz} = 0 \tag{8}$$

The expression leads to bilinear form as,

$$\left(D^2_t - D^2_x - D^4_x + \frac{1}{4}D^2_y + D_yD_t + D_xD_z\right)f{\cdot}f = 0, \tag{9}$$

Using the following transformations, we obtain

$$q = 2\ln f(x,y,z,t) \Leftrightarrow u(x,y,z,t) = c(t)q_{xx} = 6[\ln f]_{xx}. \tag{10}$$

3. Lump type solutions of Boussinesq equation

To acquire lump solutions of (9), we begin with

$$f_{lump} = \psi^2 + \xi^2 + a_9, \tag{11}$$

with

$$\begin{cases} \psi(x,y,z,t) = x + ya_1 + za_2 + ta_3 + a_4 \\ \xi(x,y,z,t) = x + ya_5 + za_6 + ta_7 + a_8 \end{cases}, \tag{12}$$

wherea_i,$(i = 1, 2, 3, ..., 9)$are constraints to be identified. By utilizing the symbolic computation tool Maple and putting (11) into (9), we attain some equations for the constraints:

Case-I:

$$\begin{cases} a_5 = a_1 + 2\sqrt{a_1a_7 - a_7^2 - 2}, a_2 = \frac{1}{2}a_7a_5 - \frac{1}{4}a_1^2, a_6 = 2 - a_1a_7 \\ -\frac{1}{2}a_1a_5 - a_2, \\ a_1 = a_7 = const., a_3 = a_4 = a_8 = a_9 = 0, \end{cases} \tag{13}$$

Inserting (13) into (11) along with (12), we get following solution,

$$f_{lump} = \left[x + a_1y + z\left(-\frac{1}{4}a_1^2 + \frac{1}{2}a_7a_5\right)\right]^2 + \left[x + ya_5 + z\left(2 - a_1a_7 - \frac{1}{2}a_1a_5 - a_2\right) + a_7t\right]^2 + a_9 \tag{14}$$

We have depicted physical representations of the solution (14) along with (10) for some values $a_1 = 1.5$, $a_7 = 2$, and $a_9 = 1$ in Fig. 1.

Case-II:

$$\begin{cases} a_1 = a_3 = a_4 = a_5 = a_7 = a_8 = const., a_2 = \chi_1 - \chi_2, a_6 = \chi_1 + \chi_2, \\ a_9 = -\dfrac{4a_1a_3a_4^2 - 4a_1a_3a_8^2 + 4a_3^2a_4^2 - 4a_4^2a_5a_7 + 4a_5a_7a_8^2 + a_4^2 + 16a_4a_8}{a_1^2 - 2a_1a_5 - 4a_1a_7 + 4a_3^2 - 4a_3a_5 - 8a_3a_7 + a_5^2 + 4a_7^2 + 8} \end{cases} \tag{15}$$

where $\chi_1 = 1 - \frac{1}{4}a_1a_5 - \frac{1}{2}a_1a_7 - \frac{1}{2}a_3a_5 - a_3a_7and\chi_2 = \frac{1}{8}a_1^2 + \frac{1}{2}a_3a_1 + \frac{1}{2}a_3^2 - \frac{1}{8}a_5^2 - \frac{1}{2}a_7a_5 - \frac{1}{2}a_7^2$

Replacing (15) into (11) along with (12), yields the following solution,

$$f_{lump} = \{x + a_1y + z(\chi_1 - \chi_2) + a_3t + a_4\}^2 + \{x + a_5y + z(\chi_1 + \chi_2) + a_7t + a_8\}^2 - \frac{4a_1a_3a_4^2 - 4a_1a_3a_8^2 + 4a_3^2a_4^2 - 4a_4^2a_5a_7 + 4a_5a_7a_8^2 + a_4^2 + 16a_4a_8}{a_1^2 - 2a_1a_5 - 4a_1a_7 + 4a_3^2 - 4a_3a_5 - 8a_3a_7 + a_5^2 + 4a_7^2 + 8} \tag{16}$$

We have depicted physical representations (see Fig. 2) of the solution (16) along with (10) for $a_1 = 1.5$, $a_3 = 0.2$, $a_4 = 1$, $a_5 = 0.5$, $a_7 = 0.2$and$a_8 = -0.5$. Fig. 2 presents a 3D view of the lump solution of (2) in various planes along with the corresponding contour shape. It is seen that Fig. 2 resembles an eye-shaped lump wave profile, consisting of two valleys and a central hump. Moreover, it is noted that the lump wave has the uppermost crest relative to its adjacent area and can occur within a brief period.

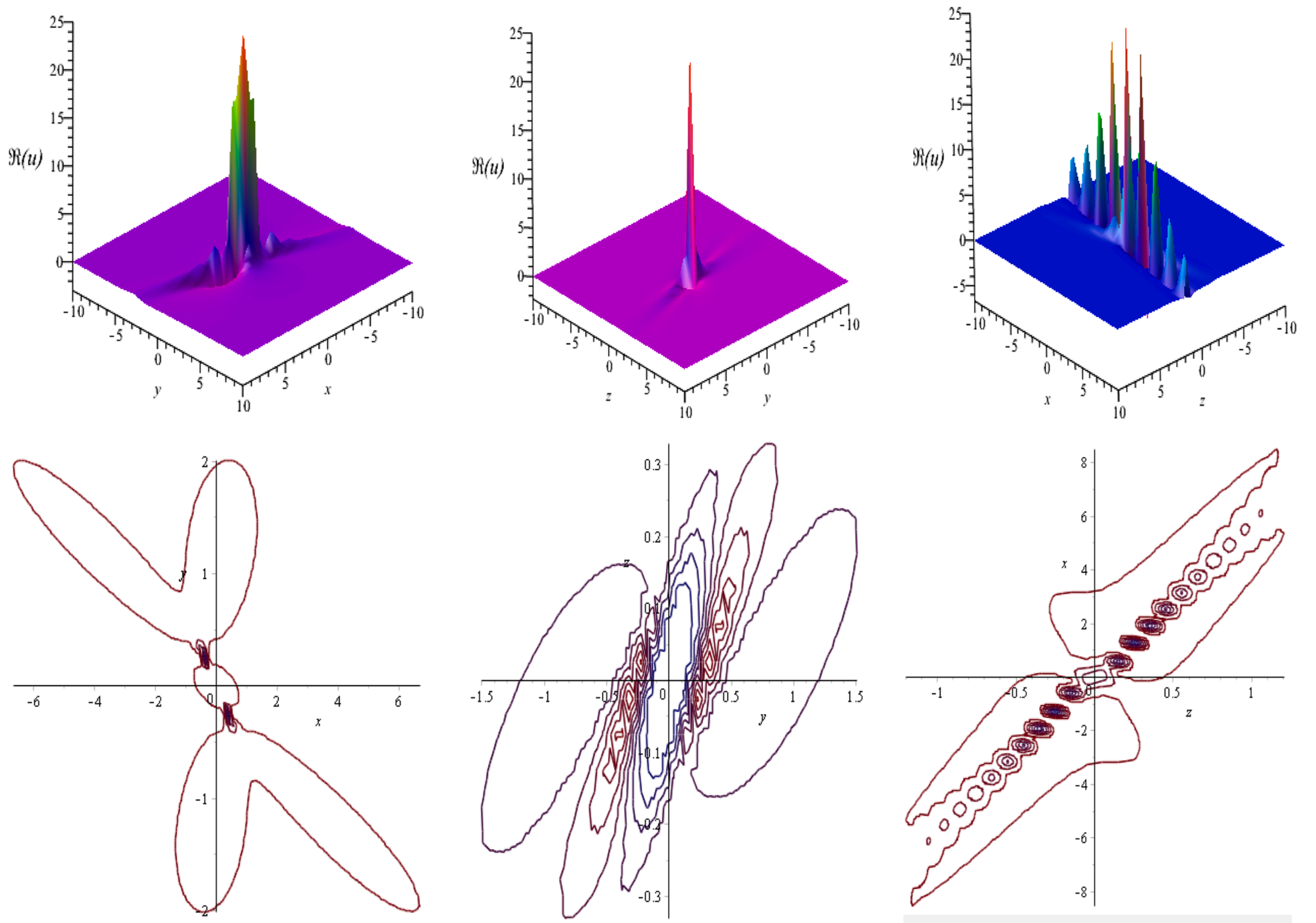

(a) (b) (c)

Fig. 1. Lump solution of (14) by picking appropriate parameters: $a_1 = 1.5$, $a_7 = 2$, and$a_9 = 1$, 3D plots at $t = 0$ with (a)$z = 0$ (b)$x = 0$ (c)$y = 0$and relative contour shapes (bottom) respectively.

4. Multiple soliton solutions and their hybrid structures

Generally, the soliton solutions can be discovered through applying Hirota's scheme.[42] Consider that f exhibits multi-solitons in the form:

$$f = f_M = \sum_{\varepsilon=0,1} \exp\left(\sum_{i=1}^{M} \varepsilon_i \varpi_i + \sum_{i<j}^{M} \varepsilon_i \varepsilon_j C_{ij} \right) \tag{17}$$

4.1. The 2-soliton solutions and their distorted structures

We take $M = 2$, so f_2 is derived as

$$f_2 = 1 + e^{\vartheta_1} + e^{\vartheta_2} + C_{12} e^{\vartheta_1 + \vartheta_2}, \tag{18}$$

wherein,

$$\vartheta_i = k_i(x + p_i y + q_i z + r_i t) + \vartheta_i^0, \tag{19}$$

By replacing (18) into (9) and over-simplifications, then set all the coefficients of exponential terms as zero, which leads to the following solution:

$$q_i = k_i^2 - \frac{1}{4} p_i^2 - p_i r_i - r_i^2 + 1 (i = 1, 2), \qquad C_{12} = \frac{\sigma - 24k_1k_2}{\sigma + 24k_1k_2}, \tag{20}$$

where, $\sigma = 12k_1^2 + 12k_2^2 + p_1^2 - 2p_1p_2 + 4p_1r_1 - 4p_1r_2 + p_2^2 - 4p_2r_1 + 4p_2r_2 + 4r_1^2 - 8r_1r_2 + 4r_2^2$.

Then inserting (18) into (10) with (20), we attain the two-soliton wave of (2). If letting $k_1 = 1, k_2 = 2, r_1 = r_2 = 1, p_1 = 1, p_2 = 2$and $\vartheta_1^0 = \vartheta_2^0 = 0$, we can attain a two-kink wave is portrayed in Fig. 3(a).

Using the above method, Eq. (18) generates breather wave by selecting appropriate constraints. These breather waves of (2) can be obtained from (20) for the following requirements:

$$k_1 = Ib_1, k_2 = -Ib_2, p_1 = a_1, p_2 = -a_1, r_1 = b_1, r_2 = b_1. \tag{21}$$

For instance, choosing constraints as $k_1 = k_2^* = I, p_1 = -p_2 = 1.5, r_1 = r_2 = 1, \vartheta_1^0 = \vartheta_2^0 = 0$, we can attain breather solutions which is illustrated in Fig. 3(b). Additionally, Eq. (18) can be expressed as:

$$f = 1 + \exp\{(1.5y - 1.5z)I\}\{2\cos(x + 1.5625z + t) + 1\} \tag{22}$$

and thus

$$u = 6[\ln(1 + \{2\cos(x + 1.5625z + t) + 1\}\exp\{(1.5yI - 1.5zI)I\})]_{xx} \tag{23}$$

The waveforms presented in (23), exhibit bullet-shaped twofold periodic waves, as seen in Fig. 3(c). However, by setting the parameters as $k_1 = k_2^* = I, p_1 = p_2^* = 1.5I, r_1 = r_2 = 1, \vartheta_1^0 = \vartheta_2^0 = 0$, Eq. (18) simplifies to

$$f = 1 + (6.333333333 - I)\exp(-3y + 3z) + 2\cos(x - 0.4275z + t)\exp(-1.5y + 1.5z) \tag{24}$$

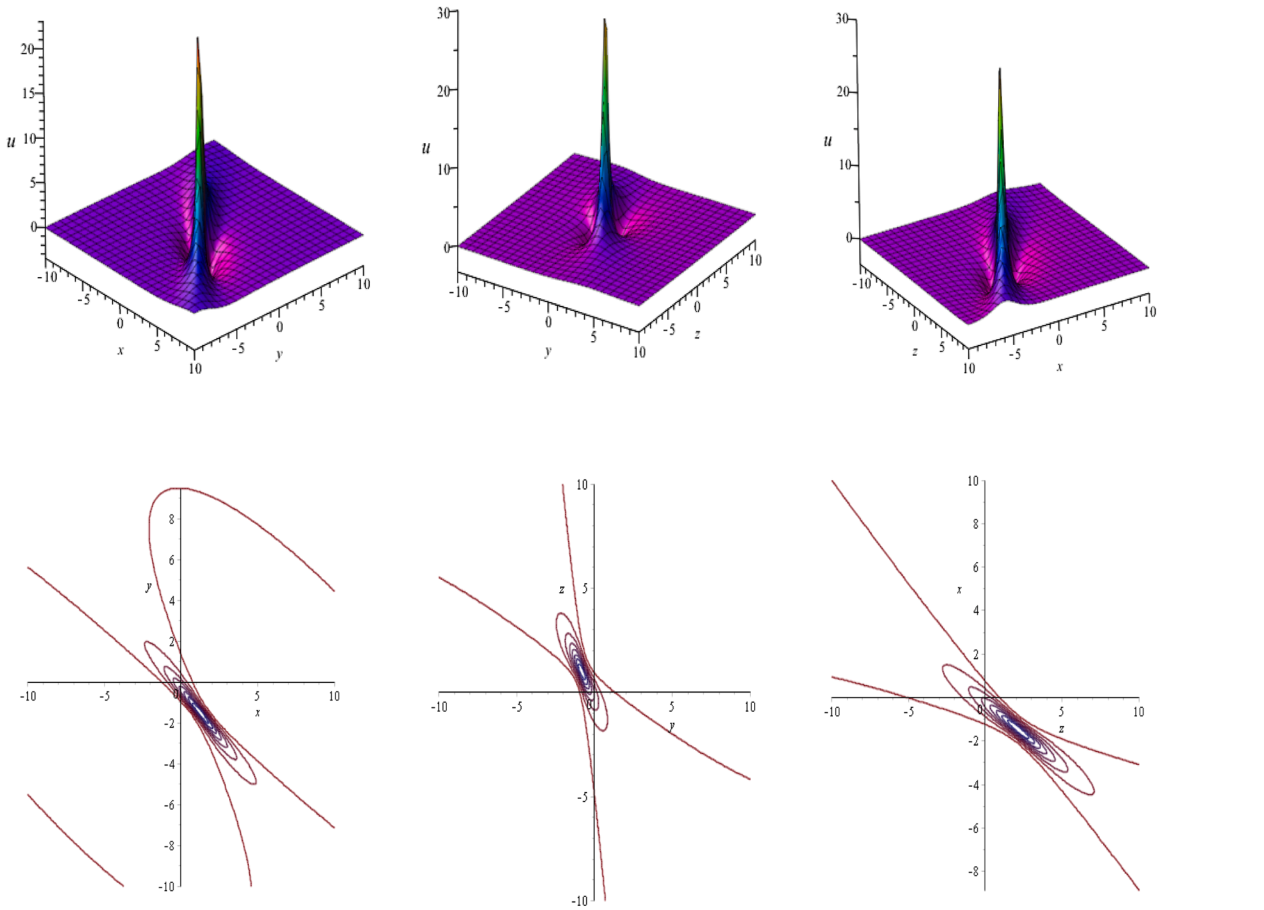

(a) (b) (c)

Fig. 2. Lump solution of (16) by taking suitable parameters: $a_1 = 1.5$, $a_3 = 0.2$, $a_4 = 1$, $a_5 = 0.5$, $a_7 = 0.2$and$a_8 = -0.5$, 3D plots at $t = 0$ with (a) $z = 0$ (b) $x = 0$ (c) $y = 0$and corresponding contour plots (bottom) respectively.

and thus

$$u = 6[\ln(1 + 2\cos(x - 0.4275z + t)\exp(-1.5y + 1.5z) +(6.333333333 - I)\exp(-3y + 3z))]_{xx} \tag{25}$$

The solution profile given by Eq. (25), illustrates periodic line lump waves, as exposed in Fig. 3(d).

4.2. The 3-solitons solutions and their distorted structures

We consider $M = 3$, so $f_3$is derived as

$$f_3 = 1 + e^{\vartheta_1} + e^{\vartheta_2} + e^{\vartheta_3} + C_{12}e^{\vartheta_1+\vartheta_2} + C_{13}e^{\vartheta_1+\vartheta_3} + C_{23}e^{\vartheta_2+\vartheta_3} + C_{12}C_{23}C_{13}e^{\vartheta_1+\vartheta_2+\vartheta_3}, \tag{26}$$

where, $\vartheta_i = k_i(x + p_i y + q_i z + r_i t) + \vartheta_i^0, (1 \le i \le 3)$,and q_i, C_{ij}in which $j > i$; $i, j = 1, 2, 3$derives from (17).

For parameter $r_1 = r_2 = r_3 = 1$, $k_1 = k_2 = k_3 = 2$, $p_1 = 1$, $p_2 = 2$, $p_3 = -1$ and $\vartheta_1^0 = \vartheta_2^0 = \vartheta_3^0 = 0$, leads to the collision of 3-bell solitons, as depicted in Fig. 4(a) with contour plot Fig.(b). This figure shows the interaction between three bell-shaped solitons, which act together at (0, 0).

In addition, by taking the parameters $r_1 = r_2 = 1, r_3 = -1, k_1 = k_2^* = I, k_3 = 1, p_1 = 1, p_2 = -2, p_3 = -1$ and $\vartheta_1^0 = \vartheta_2^0 = \vartheta_3^0 = 0$, then (26) reduces to

$$f = \begin{cases} 1 + 2e^{i\left(\frac{3}{2}y - \frac{9}{8}z\right)}\cos\left(x - \frac{1}{2}y - \frac{9}{8}z + t\right) - \frac{13}{3}e^{i\left(3y - \frac{9}{4}z\right)} \\ +e^{x-y-\frac{1}{4}z-t}\left[1 + \left(\frac{5}{13} - \frac{12}{13}i\right)e^{i\left(x+y-\frac{9}{4}z+t\right)} + \left(-\frac{55}{73} + \frac{48}{73}i\right)e^{-i(x-2y+t)}\right. \\ \left.-\left(\frac{301}{219} + \frac{300}{73}i\right)e^{i\left(3y-\frac{9}{4}z\right)}\right] \end{cases} \tag{27}$$

This is a solution with complex values, where both the real and imaginary components represent the collision between a periodic wave at that point a periodic line lump upsurge, where the lump upsurge emerging along the diagonal. We have portrayed physical illustrations of the solution (27) in Fig. 4(c).

For the values $k_1 = k_2^* = 2I, k_3 = 1, p_1 = p_2^* = I, p_3 = -1, r_1 = r_2 = 1$, $r_3 = -1$and $\vartheta_1^0 = \vartheta_2^0 = \vartheta_3^0 = 0$, then (26) reduces to

$$f = \begin{cases} 1 + e^{x-y-\frac{1}{4}z-t} + 49e^{-4y+4z} + 2e^{-2y+2z}\cos\left(2x - \frac{15}{2}z + 2t\right) \\ -\frac{1030}{877}e^{x-3y+\frac{7}{4}z-t}\cos\left(2x - \frac{15}{2}z + 2t\right) \\ -\frac{576}{877}e^{x-3y+\frac{7}{4}z-t}\sin\left(2x - \frac{15}{2}z + 2t\right) + \frac{19453}{877}e^{x-5y+\frac{15}{4}z-t} \end{cases} \tag{28}$$

It is also complex valued solution. It represents interface amongst a

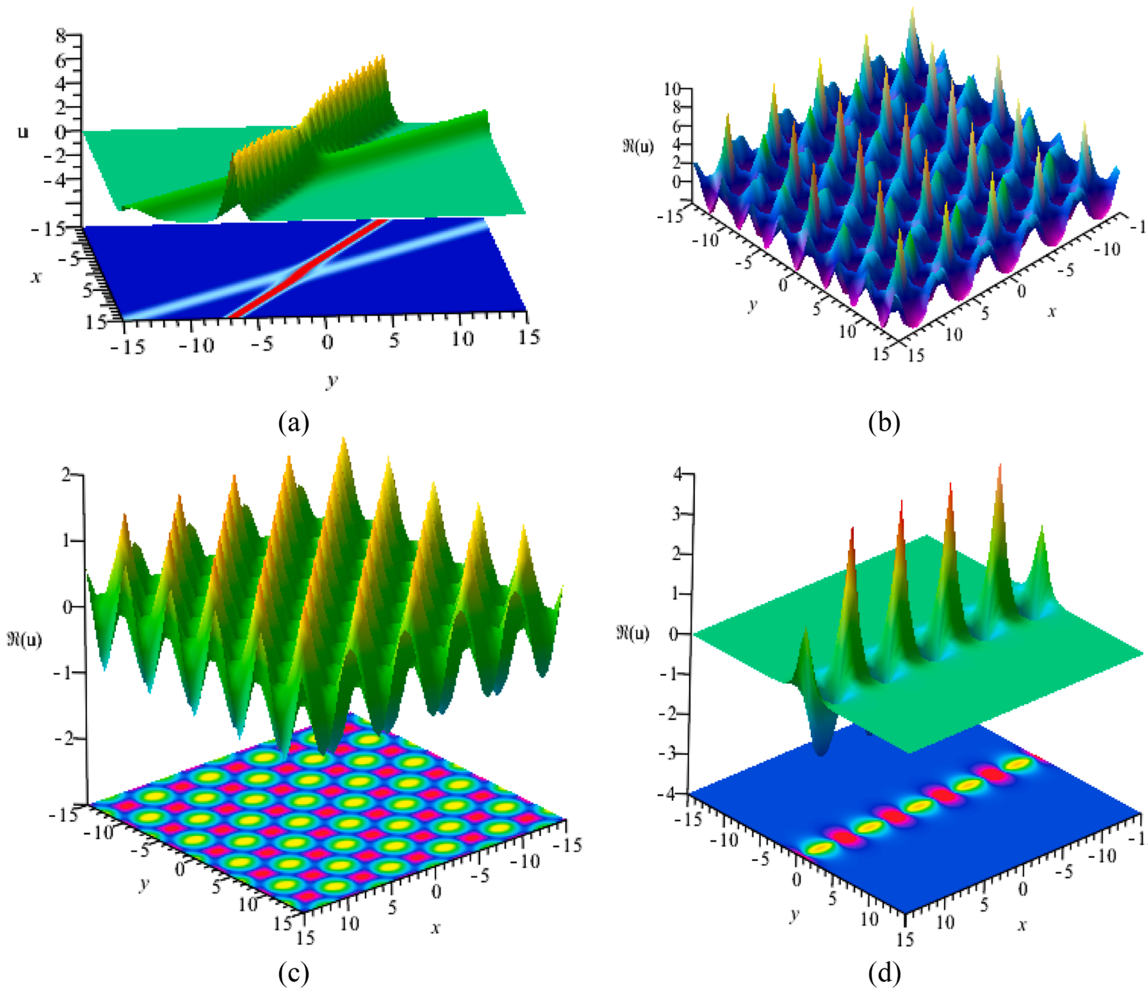

Fig. 3. (a) Collision between two bell solitons of (2) (3D view on top, density plot below), (b) Breather wave solutions of (2) for: $k_1 = k_2^* = I, p_1 = -p_2 = 1.5, r_1 = r_2 = 1$, $\vartheta_1^0 = \vartheta_2^0 = 0$, at $t = 0$; (c) Real part of the twofold periodic wave for (22) (3D view on top, density plot below), (d) Periodic line lump waves for (24) (3D view on top, density plot below).

periodic lump wave, in addition a bell soliton, where the bell soliton propagates along the diagonal and periodic lump wave transmits across the x-axis. We have portrayed physical illustrations of the solution (28) in Fig. 4(d).

4.3. The 4-solitons solutions and their distorted structures

We take $M = 4$, so $f_4$is derived as

$$f_4 = \begin{cases} 1 + e^{\vartheta_1} + e^{\vartheta_2} + e^{\vartheta_3} + e^{\vartheta_4} + C_{12}e^{\vartheta_1+\vartheta_2} + C_{13}e^{\vartheta_1+\vartheta_3} + C_{14}e^{\vartheta_1+\vartheta_4} + C_{23}e^{\vartheta_2+\vartheta_3} \\ + C_{24}e^{\vartheta_2+\vartheta_4} + C_{34}e^{\vartheta_3+\vartheta_4} + C_{12}C_{23}C_{13}e^{\vartheta_1+\vartheta_2+\vartheta_3} + C_{12}C_{24}C_{14}e^{\vartheta_1+\vartheta_2+\vartheta_4} \\ + C_{13}C_{14}C_{34}e^{\vartheta_1+\vartheta_3+\vartheta_4} + C_{23}C_{24}C_{34}e^{\vartheta_2+\vartheta_3+\vartheta_4} + C_{12}C_{23}C_{34}e^{\vartheta_1+\vartheta_2+\vartheta_3+\vartheta_4} \end{cases}, \tag{29}$$

where, $\vartheta_i = k_i(x + p_i y + q_i z + r_i t) + \vartheta_i^0, (1 \le i \le 4)$,and q_i, C_{ij}in which $i < j$; $i, j = (1, \ldots, 4)$originates from (17).

For the principles $k_1 = 1, k_2 = k_3 = 2, k_4 = -2, p_1 = p_3 = 1, p_2 = 2, p_4 = -1.2, r_1 = 1, r_2 = -1, r_3 = 1.2, r_4 = 2$and $\vartheta_1^0 = \vartheta_2^0 = \vartheta_3^0 = \vartheta_4^0 = 0$, yield collision of four-bell soliton solutions, as revealed in Fig. 5. Fig. 5(a) elucidates the interaction of four bell-shaped solitons, which collide at (0, 0). We also present the corresponding contour plot with different color schemes for enhanced clarity.

Additionally, when the values $k_1 = k_2^* = I, k_3 = 1, k_4 = 2, p_1 = p_2^* = I, p_3 = 1, p_4 = 2, r_1 = r_2 = r_4 = 1$, $r_3 = 2$and $\vartheta_1^0 = \vartheta_2^0 = \vartheta_3^0 = \vartheta_4^0 = 0$, then Eq. (29) reduces to

$$\begin{aligned} f = {} & 1 + 2e^{-y+z}\cos\beta_1 + e^{\beta_2} + e^{\beta_3} + \frac{13}{109}e^{\beta_4} + 13e^{-2y+2z} + e^{\beta_5}\left\{ -\frac{238}{97}\cos\beta_1 + \frac{192}{97}\sin\beta_1 \right\} \\ & + e^{\beta_6}\left\{ -\frac{6971926}{36550861}\cos\beta_1 + \frac{13498368}{36550861}\sin\beta_1 \right\} + e^{\beta_7}\left\{ -\frac{1534}{3457}\cos\beta_1 + \frac{7488}{3457}\sin\beta_1 \right\} \\ & + \frac{3133}{97}e^{x-y-\frac{9}{4}z+2t} + \frac{54925}{3457}e^{2x+2y+4z+2t} + \left(-\frac{20111}{10573} + \frac{16224}{10573}i \right) e^{3x+3y-\frac{1}{4}z+4t}, \end{aligned} \tag{30}$$

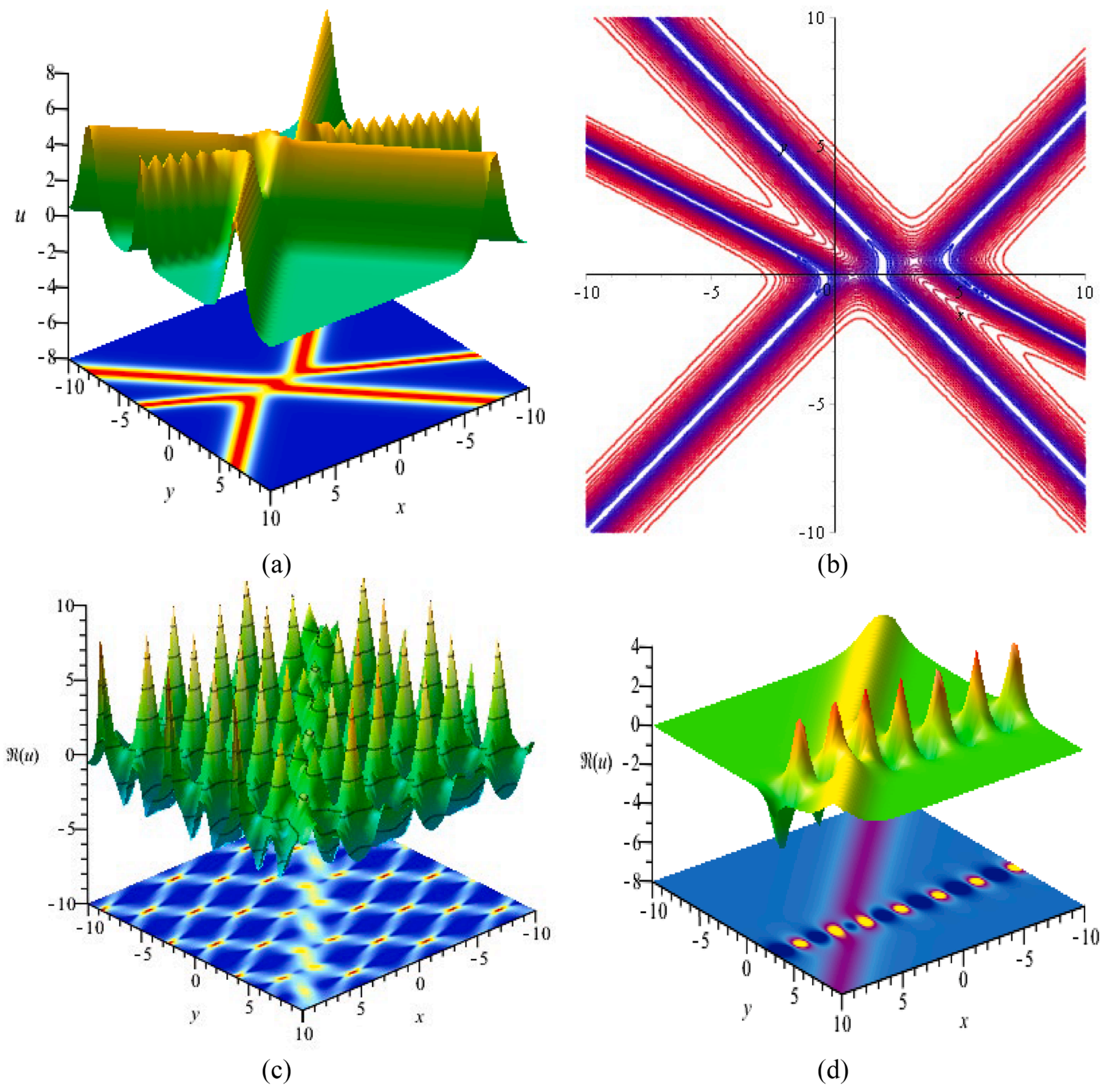

Fig. 4. (a) Collision of three bell solitons via (26) at $t = 0$, $z = 0$; (b) contour plot corresponding to (a), (c) collision between a periodic line lump trend as well as periodic wave, as determined by the solution of (27) (3D view on top, density plot on the bottom), (d) collision between a bell soliton and a periodic line lump wave utilizing (27) at $t = 0$, $z = 2$; (3D view on top, density plot on the bottom).

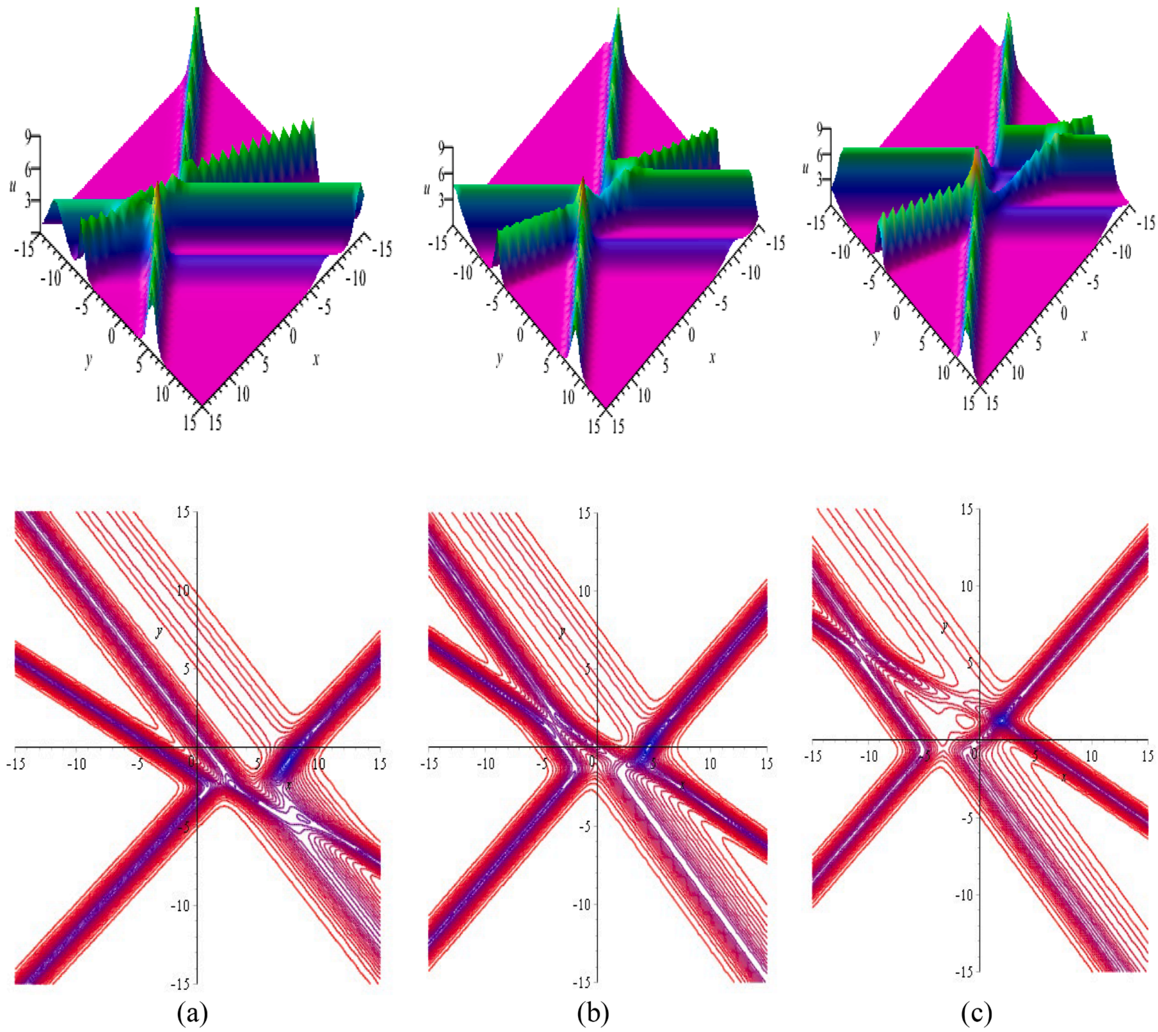

Fig. 5. The collision of four bell solitons through (26) 3D view at $z = 0$, (a) $t = -2$; (b) $t = 0$; (c) $t = 2$; silhouette plots of the corresponding 3D view (bottom) respectively.

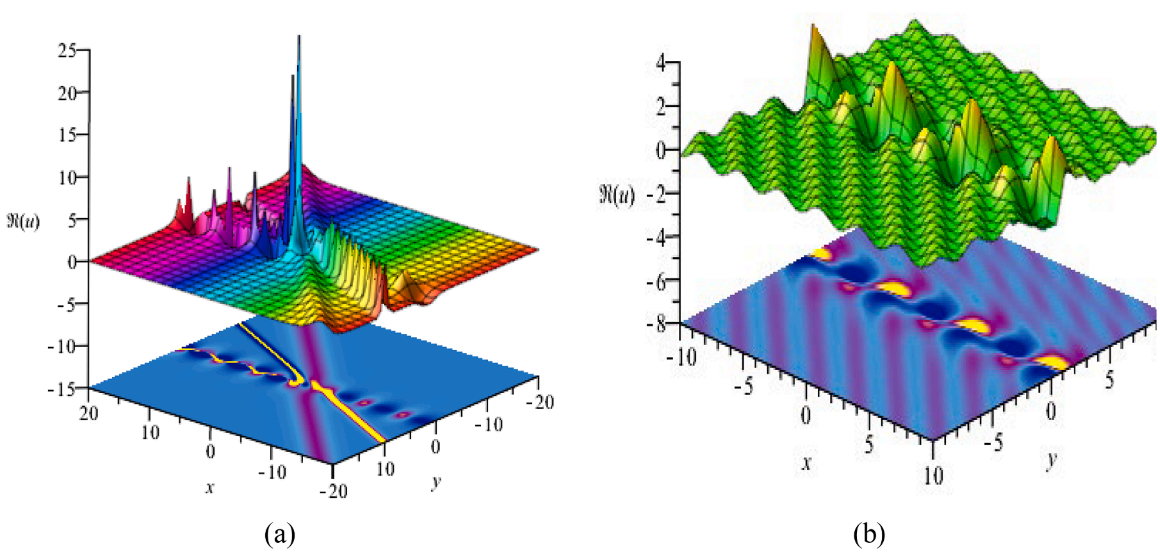

Fig. 6. (a) Collision among periodic wave, bell soliton, and a periodic line lump wave through (30) (3D plot on top, density plot below), (b) Collision of a paired periodic wave with a periodic line lump wave for (31) (3D plot on top, density plot below).

where,-
$\beta_1 = x - \frac{3}{4}z + t, \beta_2 = x + y - \frac{17}{4}z + 2t, \beta_3 = 2x + 4y + 2z + 2t, \beta_4 = 3x + 5y - \frac{9}{4}z + 4t, \beta_5 = x - \frac{13}{4}z + 2t, \beta_6 = 3x + 4y - \frac{5}{4}z + 4t, \beta_7 = 2x + 3y + 3z + 2t.$

The real and imaginary components of this complex-valued result show how a periodic wave, a periodic line lump wave, and a bell-like soliton interact. In this interaction, the bell soliton appears along the diagonal, while the lump waves are aligned along the x-axis. We have depicted physical representations of the solution (30) in Fig. 6(a).

For the values $k_1 = k_2^* = I, k_3 = k_4^* = 2I, p_1 = p_2^* = I, p_3 = 1, p_4 = 2, r_1 = r_4 = 1, r_2 = -1, r_3 = 2$and $\vartheta_1^0 = \vartheta_2^0 = \vartheta_3^0 = \vartheta_4^0 = 0$,Eq. (29) written as

$$f = 1 + e^{2i\gamma_1} + e^{-2i\gamma_2} - 191e^{2i\gamma_3} + e^{-y+z}\left\{\begin{array}{l} e^{i\gamma_4} + \left(\frac{961}{97} - \frac{384}{97}i\right)e^{i\gamma_5} + \left(\frac{109}{2509} + \frac{144}{2509}i\right)e^{i\gamma_6} + \\ \left(-\frac{394145}{3138} - \frac{603923}{7972}\right)e^{i\gamma_7} \end{array}\right\}$$
$$+e^{-y-z}\left\{e^{-i\gamma_8} + \left(-\frac{1535}{5473} - \frac{1152}{5473}i\right)e^{-i\gamma_9} + \left(-\frac{491}{373} + \frac{336}{373}i\right)e^{-i\gamma_{10}} + \left(-\frac{509429}{4773} - \frac{36965}{7922}i\right)e^{-i\gamma_{11}}\right\} \tag{31}$$
$$+e^{-2y}\left\{\begin{array}{l} \left(-\frac{11}{25} + \frac{48}{25}i\right)e^{i2t} + \left(\frac{261243}{1189} + \frac{1716635}{3074}i\right)e^{2i\gamma_{12}} + \left(\frac{19296}{163763} - \frac{22474}{116421}i\right)e^{2i\gamma_{13}} \\ + \left(\frac{47441}{13706} - \frac{49243}{7569}i\right)e^{-2i\gamma_{14}} \end{array}\right\}$$

where,

$$\gamma_1 = x + y - \frac{37}{4}z + 2t, \gamma_2 = x + 2y - 7z + t, \gamma_3 = -y - \frac{9}{4}z + t, \gamma_4 = x - \frac{3}{4}z + t, \gamma_5 = -x - 4y + \frac{53}{4}z - t,$$
$$\gamma_6 = 3x + 2y - \frac{77}{4}z + 5t, \gamma_7 = x - 2y + \frac{21}{4}z + 3t, \gamma_8 = x - \frac{3}{4}z - t, \gamma_9 = 3x + 4y - \frac{59}{4}z + t,$$
$$\gamma_{10} = -x - 2y + \frac{71}{4}z - 5t, \gamma_{11} = x + 2y + \frac{15}{4}z - 3t, \gamma_{12} = -y - \frac{9}{4}z + 2t, \gamma_{13} = x + y - \frac{37}{4}z + 3t, \gamma_{14} = x + 2y - 7z$$

This is a complex-valued solution, where both the real and imaginary portions illustrate the collision between paired periodic wave and periodic line lump wave, while lump wave positioned along the x-axis. Inside Fig.−6(b), we portrayed the physical representations solution of Eq. (31).

5. Interaction aspects of integrable (3 + 1)-D Boussinesq equation

In this segment, we describe three types of interaction phenomena of (2) like (i) lump and a stripe soliton, (ii) lump, periodic upsurge, also a double stripe soliton, (iii) two double stripe solitons.

5.1. Lump and stripe soliton interaction

To get the lump and stripe soliton interaction of (2), consider f has the following form,

$$f = k_0 + k_1\Lambda_1^2 + k_2 e^{\Lambda_2} \tag{32}$$

with

$$\left\{\begin{array}{l} \Lambda_1(x, y, z, t) = xa_0 + ya_1 + za_2 + ta_3 + a_4 \\ \Lambda_2(x, y, z, t) = xb_0 + yb_1 + zb_2 + tb_3 + b_4 \end{array}\right. , \tag{33}$$

here a_i,b_i the coefficients a_i's associated with (i = 0, 1, ..., 4) serve as undefined coefficients to be calculated. By replacing Eq. (32) into Eq. (9) and using symbolic computation, we acquire some equations for the constraints:

Case-1:

$$\left\{\begin{array}{l} b_2 = \frac{1}{4}\frac{4b_0^4 + 4b_0^2 - b_1^2 - 4b_1b_3 - 4b_3^2}{b_0}, k_1 = 0, \\ a_0 = a_1 = a_2 = a_3 = a_4 = k_0 = k_2 = b_0 = b_1 = b_3 = b_4 = const. \end{array}\right. \tag{34}$$

Therefore, replacing Eq. (34) into Eq. (32), yields,

$$f = k_0 + k_2 e^{b_0x + b_1y + \frac{1}{4}\frac{z\left(4b_0^4 + 4b_0^2 - b_1^2 - 4b_1b_3 - 4b_3^2\right)}{b_0} + b_3t + b_4} \tag{35}$$

Case-2:

$$\left\{\begin{array}{l} a_1 = -2a_3, b_2 = \frac{1}{4}\frac{4b_0^4 + 4b_0^2 - b_1^2 - 4b_1b_3 - 4b_3^2}{b_0}, a_0 = a_2 = 0, \\ a_3 = a_4 = b_0 = b_1 = b_3 = b_4 = k_0 = k_1 = k_2 = const. \end{array}\right. \tag{36}$$

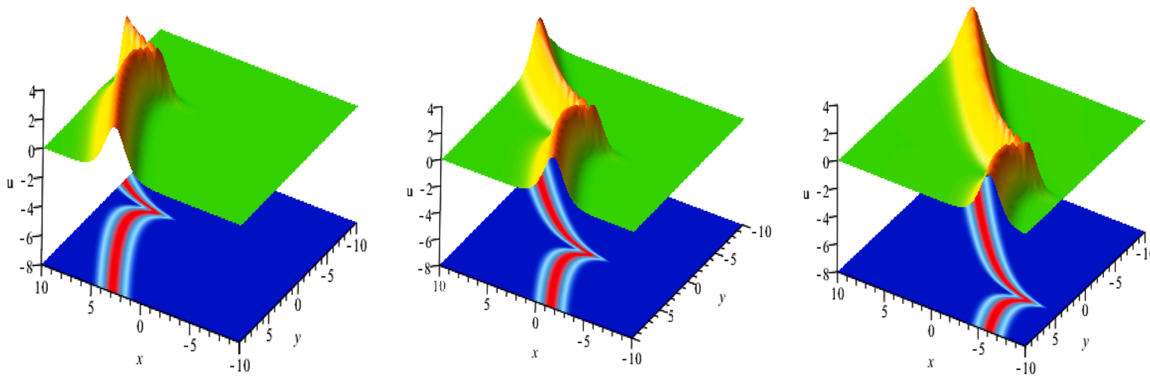

(a) (b) (c)

Fig. 7. Profile of Eq. (32) by selecting appropriate parameters: $k_1 = 1$, $k_2 = 5$, $k_3 = 2$, $a_3 = 1$, $a_4 = 2.5$, $b_0 = 1.5$, $b_1 = b_3 = 1$, $b_4 = -1$in xy − plane for $z = 0$ at (a) $t = -6$ (b) $t = 0$ and (c) $t = 6$ (3D plot on top, density plot below).

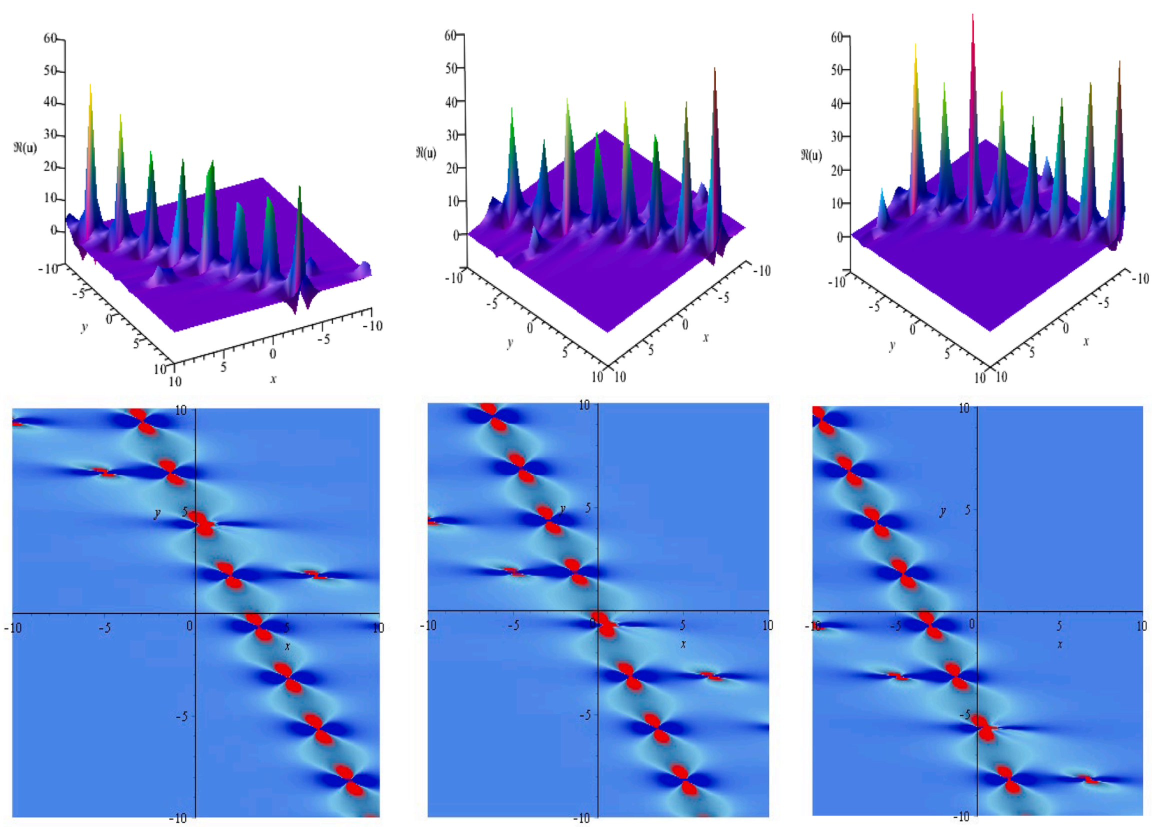

(a) (b) (c)

Fig. 8. Profile of Eq. (40) with selected parameters: $k_1 = 2.5$, $a_0 = a_1 = a_3 = 1$, $a_4 = 0.25$, $b_3 = 1.25$, $b_4 = 1.5$, 3D view with $z = 0$at (a) $t = -5$ (b) $t = 0$ and (c) $t = 5$, along with their corresponding density plots (bottom) respectively.

Therefore, replacing Eq. (36) into Eq. (32), yields,

$$f = k_0 + k_1(-2ya_3 + ta_3 + a_4)^2 + k_2 e^{b_0 x + b_1 y + \frac{1}{4}\frac{z\left(4b_0^4 + 4b_0^2 - b_1^2 - 4b_1 b_3 - 4b_3^2\right)}{b_0} + b_3 t + b_4} \tag{37}$$

The graphical representations of this solution, as shown in Eq. (37) along with Eq. (10), for the parameters as $k_1 = 1$, $k_2 = 5$, $k_3 = 2$, $a_3 = 1$, $a_4 = 2.5$, $b_0 = 1.5$, $b_1 = b_3 = 1$, $b_4 = -1$ are demonstrated in Fig. 7.

5.2. Interface of lump, periodic wave as well double stripe solitons

Consider f has the form as,

$$f = 1 + k_0 \cosh(\Lambda_3) + k_1 \cos(\Lambda_4) \tag{38}$$

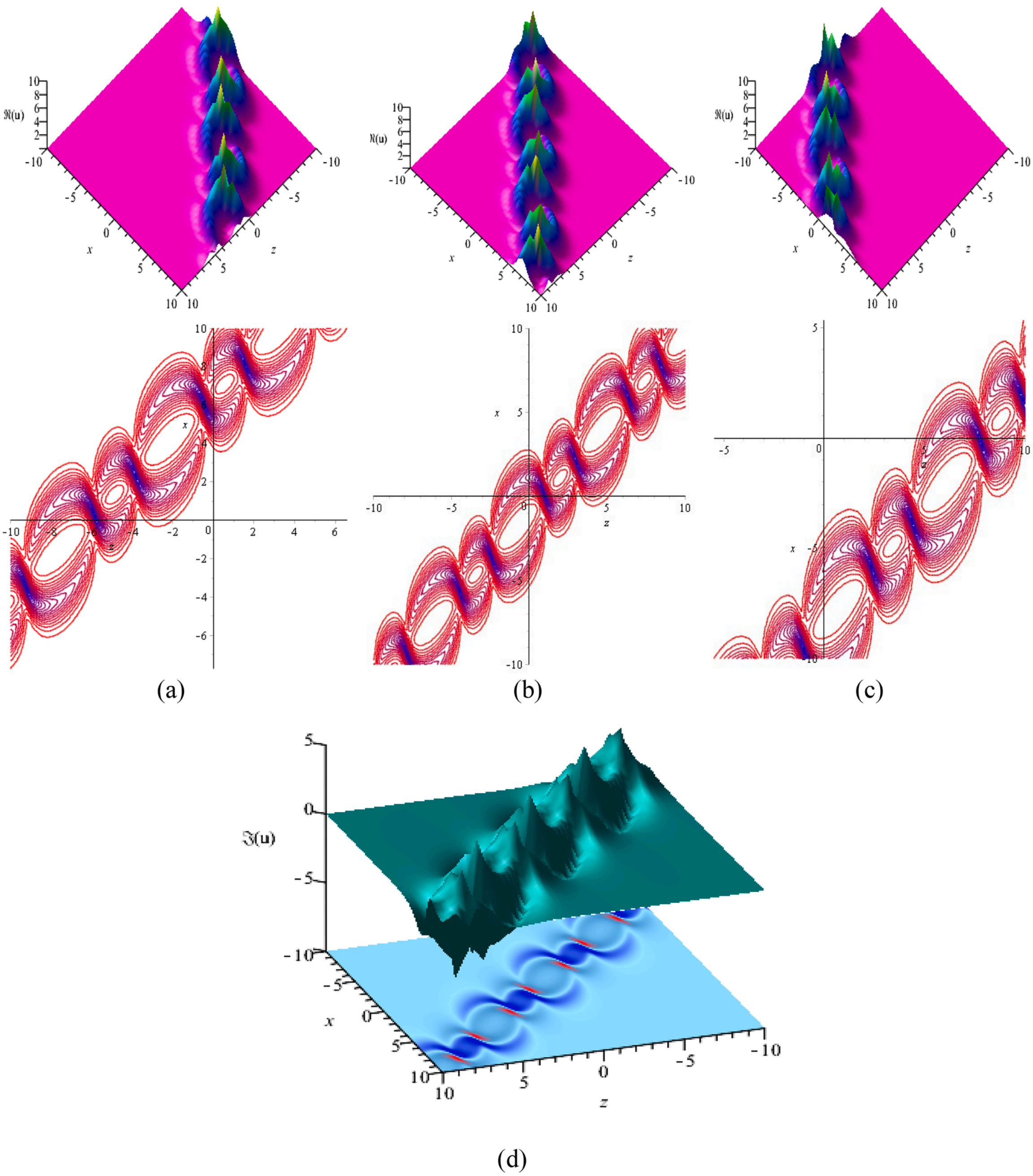

Fig. 9. Shape of (40) with selected constraints:$k_1 = 2.5$, $a_0 = a_1 = 1$, $a_3 = 1.25$, $a_4 = 1$, $b_3 = 2$, $b_4 = 1$, 3D view with $z = 0$at (a) $t = -6$ (b) $t = 0$ as well as (c) $t = 6$, with consistent contour plans (bottom) individually (d) Imaginary part of (b) (3D plot on top, density plot at the bottom).

where Λ_1 and Λ_2 are defined in (33). By replacing (38) into (9) and using symbolic calculation, we derive the following constraints equations:

$$\begin{cases} a_0=a_1=a_3=a_4=b_3=b_4=k_1=const., a_2=\frac{1}{4}\frac{4a_0^4+4a_0^2-a_1^2-4a_1a_3-4a_3^2}{a_0}, \\ b_0=\frac{\alpha}{6a_0}, b_1=-2b_3, b_2=\frac{\left(28a_0^4+4a_0^2-\frac{1}{3}a_1^2-\frac{4}{3}a_1a_3-\frac{4}{3}a_3^2\right)\alpha}{24a_0^3}, k_0=\frac{\beta k_1}{12a_0^4}, \end{cases} \tag{39}$$

with

$\alpha = \sqrt{-36a_0^4 + 3a_1^2 + 12a_1a_3 + 12a_3^2}$and

$\beta = \sqrt{144a_0^8 - a_1^4 - 8a_1^3a_3 - 24a_1^2a_3^2 - 32a_1a_3^3 - 16a_3^4}$

Therefore, replacing (39) into (38) along with (33), yields the following solution,

$$f=1+\frac{\beta k_1}{12a_0^4}\cosh\left\{a_0x+a_1y+\frac{1}{4}\frac{z\left(4a_0^4+4a_0^2-a_1^2-4a_1a_3-4a_3^2\right)}{a_0}+a_3t+a_4\right\}$$
$$+k_1\cos\left\{\frac{\alpha x}{6a_0}-2yb_3+\frac{\left(28a_0^4+4a_0^2-\frac{1}{3}a_1^2-\frac{4}{3}a_1a_3-\frac{4}{3}a_3^2\right)\alpha z}{24a_0^3}+b_3t+b_4\right\} \tag{40}$$

The graphical representations via (37) along with (10), for $k_1 = 1$, $k_2 = 5$, $k_3 = 2$, $a_3 = 1$, $a_4 = 2.5$, $b_0 = 1.5$, $b_1 = b_3 = 1$, $b_4 = -1$ are illustrated in Fig. 8.

Furthermore, a dissimilar kind of interaction arises with minor adjustments to the constraints $k_1 = 2.5$, $a_0 = a_1 = 1$, $a_3 = 1.25$, $a_4 = 1$, $b_3 =$

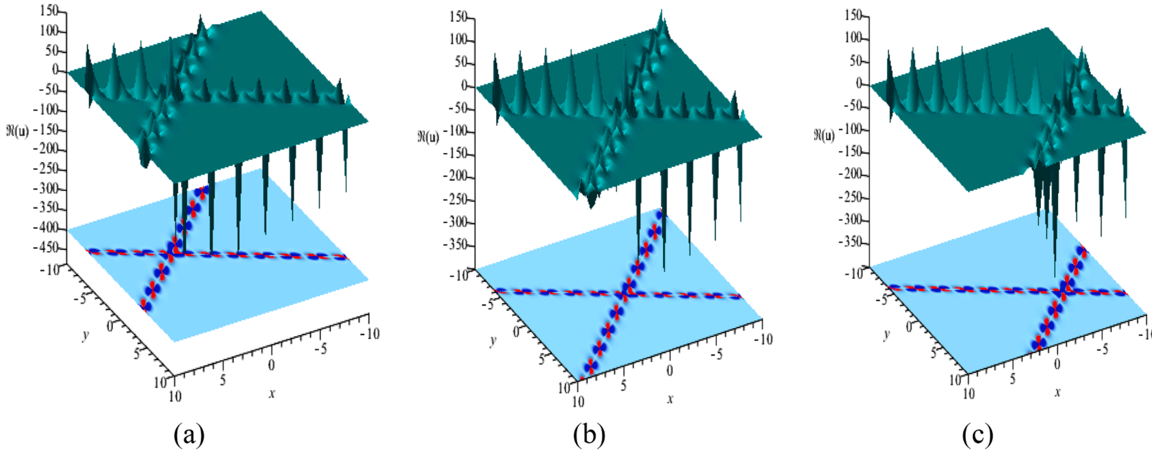

Fig. 10. Interaction of two-stripe solitons via (43) with selected parameters: $k_1 = -2.5$, $a_0 = 3$, $a_1 = 1$, $a_3 = 2$, $a_4 = 1.5$, $b_3 = 2$, $b_4 = 1$, in the xy − plane and $z = 0$ at (a) $t = -5$ (b) $t = 0$ and (c) $t = 5$, (3D upper, density plot lower).

2, $b_4 = 1$, as portrayed in Fig. 9. This figure illustrates the interactions of lump and the periodic wave.

5.3. Two double stripes soliton interaction

To get the interaction between two double stripes soliton of (2), consider f has the form as,

$$f = 1 + k_0 \sinh(\Lambda_1) + k_1 \sinh(\Lambda_2) \tag{41}$$

where Λ_1 and Λ_2 are well-defined in (33). By inserting (41) into (9) and applying symbolic computation, we obtain the resulting equations for the constraints:

$$\begin{cases} a_0 = a_1 = a_3 = a_4 = b_3 = b_4 = k_1 = const., a_2 = \dfrac{4a_0^4 + 4a_0^2 - a_1^2 - 4a_1a_3 - 4a_3^2}{4a_0}, b_0 = \dfrac{\gamma}{6a_0}, \\ b_1 = -2b_3, b_2 = -\dfrac{\left(4a_0^4 - 4a_0^2 + \frac{1}{3}a_1^2 + \frac{4}{3}a_1a_3 + \frac{4}{3}a_3^2\right)\gamma}{24a_0^3}, k_0 = \dfrac{I(12a_0^4 + a_1^2 + 4a_1a_3 + 4a_3^2)k_1}{12a_0^4} \end{cases} \tag{42}$$

with

$$\gamma = \sqrt{-36a_0^4 - 3a_1^2 - 12a_1a_3 - 12a_3^2}$$

Therefore, replacing (42) into (41) with (33), we acquire the following result,

$$f = 1 + k_1 \sinh\left(\frac{\gamma x}{6a_0} - 2yb_3 - \frac{\left(4a_0^4 - 4a_0^2 + \frac{1}{3}a_1^2 + \frac{4}{3}a_1a_3 + \frac{4}{3}a_3^2\right)\gamma z}{24a_0^3} + b_3t + b_4\right) + \frac{I(12a_0^4 + a_1^2 + 4a_1a_3 + 4a_3^2)k_1}{12a_0^4} \sinh\left(a_0x + a_1y + \frac{1}{4}\frac{z(4a_0^4 + 4a_0^2 - a_1^2 - 4a_1a_3 - 4a_3^2)}{a_0} + a_3t + a_4\right) \tag{43}$$

We present graphical representations of the solution (43) along with (10) for $k_1 = -2.5$, $a_0 = 3$, $a_1 = 1$, $a_3 = 2$, $a_4 = 1.5$, $b_3 = 2$, $b_4 = 1$ in Fig. 10. From the figure, it is observed that two couple of bell solitons transform into a periodic lump wave.

6. Important and innovation

In nonlinear chastisement, wave propagation into shallow water is a persistently inspected province. The innovative creations are:

(a) As the new higher BqE contained multi-dimensional occurrences, It's explore novel communicating interaction among diverse wave pattern in the marine engineering.
(b) New Hirota bilinear structure of the model is established by bilinear differential form, which can be applied to cover all possible single-, multi-soliton even interaction among various waves of the previous literature.
(c) This research newly established wave pattern affords precise analytical solutions for new model as commerce of lump, periodic wave, double stripe-solitons, two double stripes soliton interaction, relations of lump, the periodic wave, interaction of two-stripe solitons, making it possible to explore all incident wave dynamics in relevant field of study in soliton theory.

(d) Conveyed studies have been directed on the Boussinesq-type models in fluid mechanism as well as plasma physics. Sundry investigators have observed into the $(3+1)$-dimensional Boussinesq-type model, that is given above, in a challenge to recovering recognize gravity surfs on the superficial of water.

7. Conclusion

We have successfully examined a novel integrable (3+1)-D Boussinesq model that asserts processing of accurate solutions for collisions of exponentially restricted structures. We achieved the lump, breather, solitary, and massive colliding-wave solutions amongst the solutions by taking advantage of the Hirota bilinear structure. Such collision wave solutions can be caused by relationships among bell soliton and double periodic lump waves, lump and bell soliton, lump, periodic and two bell solitons, and interaction of double stripe waves. Analyzing the results shows that it is possible to understand complex physical phenomena of the Boussinesq model with adequate graphical representations. The obtained results showed that the enforced inquiry procedure supports a straightforward and easy methodical approach to address any nonlinear damage that occurs in engineering and applied problems while using the bilinear method.

Our findings contribute new insights to the field, revealing dynamic properties and interactions not previously documented. This research not only enhances the understanding of the (3+1)-D Boussinesq equation but also opens avenues for further studies in nonlinear wave theory.

Data availability

This article incorporates all of the data produced or examined during this investigation.

CRediT authorship contribution statement

M. Belal Hossen: Conceptualization, Investigation, Writing – original draft. **Md. Towhiduzzaman:** Data curation, Software. **Mst. Shekha Khatun:** Validation. **Harun-Or- Roshid:** Formal analysis, Project administration, Supervision. **Md. Amanat Ullah:** Investigation, Software.

Declaration of competing interest

The authors declare that they have no known competing financial interests or personal relationships that could have appeared to influence the work reported in this paper.

References

1. Khater MA, Akbar MA, Akinyemi L, Inc M. Bifurcation of new optical solitary wave solutions for the nonlinear long-short wave interaction system via two improved models of expansion method. *Opt Quantum Electron*. 2021;53:507.
2. Matveev VB, Salle MA. *Darboux Transformations and Solitons*. Berlin: Springer; 1991.
3. Shakeel M, Mohyud-din ST, Iqbal MA. Modified extended exp-function method for a system of nonlinear partial differential equations defined by seismic sea waves. *Pramana J Phys*. 2018;91:28.
4. Ullah MA, Hossen MB, Husna S. A study on exact solution of an Integrable Generalized Hirota-Satsuma equation of (2+1)-Dimensions via Exp (-Φ(ξ))-expansion method. *Int J Sci Res Eng Dev*. 2020;3(1):620–626.
5. Kumar D, Seadawy AR, Joardar AK. Modified Kudryashov method via new exact solutions for some conformable fractional differential equations arising in mathematical biology. *Chin J Phys*. 2018;56(1):75–85.
6. Han L, Bilige S, Wang X, Li M, Zhang R. Rational wave solutions and dynamics properties of the Generalized (2 + 1)-Dimensional Calogero-Bogoyavlenskii-Schiff equation by using bilinear method. *Adv Math Phys*. 2021, 9295547. Article ID.
7. Roshid HO, Ma WX. Dynamics of mixed lump-solitary waves of an extended (2+1)-dimensional shallow water wave model. *Phys Lett A*. 2018;382(45):3262–3268.
8. Hossen MB, Roshid HO, Ali MZ, Rezazadeh H. Novel dynamical behaviors of interaction solutions of the (3 + 1)-dimensional generalized B-type Kadomtsev-Petviashvili model. *Phys Scr*. 2021;96, 125236.
9. Chen HT, Zhang HQ. New multiple soliton-like solutions to the Generalized (2+1)-dimensional KP equation. *Appl Math Comput*. 2004;157:765–773.
10. Hossen MB, Roshid HO, Ali MZ. Modified double sub-equation method for finding complexiton solutions to the (1+1) Dimensional nonlinear evolution equations. *Int J Appl Comput Math*. 2017;3(3):1–19.
11. Mofarreh F, Khan A, Shah R, Abdeljabbar A. A comparative analysis of fractional order Fokker-Planck equation. *Sym*. 2023;15(2):430.
12. Roshid HO, Roshid MM, Abdeljabbar A, Begum M, Bashar H. Abundant dynamical solitary waves through Kelvin-Voigt fluid via the truncated M-fractional Oskolkov model. *Results Phys*. 2023;55, 107128.
13. Islam Z, Sheikh MAN, Roshid HO, Abdeljabbar A. Stability and spin solitonic dynamics of the HFSC model: effects of neighboring interactions and crystal field anisotropy parameters. *Opt Quant Electron*. 2024;56:190.
14. Han C, Lü X. Novel patterns in the space variable fractional order Gray–Scott model. *Nonlinear Dyn*. 2024;112:16135–16151.
15. Zhang RF, Bilige S. Bilinear neural network method to obtain the exact analytical solutions of nonlinear partial differential equations and its application to p-gBKP equation. *Nonlinear Dyn*. 2019;95:3041–3048.
16. Zhang RF, Li MC. Bilinear residual network method for solving the exactly explicit solutions of nonlinear evolution equations. *Nonlinear Dyn*. 2022;108:521–531.
17. Hossen MB, Roshid HO, Ali MZ. Characteristics of the solitary waves and rogue waves with interaction phenomena in a (2+1)-dimensional Breaking Soliton equation. *Phys Lett A*. 2018;382(19):1268–1274.
18. Zhang Y, Lü X. Data-driven solutions and parameter discovery of the extended higher-order nonlinear Schrödinger equation in optical fibers. *Physica D: Nonlinear Phenomena*. 2024;468, 134284.
19. Lou SY, Tang XY. *Nonlinear Mathematical Physics Method*. Beijing: Science Press; 2006.
20. Ma WX. Lump solutions to the Kadomtsev-Petviashvili equation. *Phys Lett A*. 2015; 379:1975–1978.
21. Imai K. Dromion and lump solutions of the Ishimori-I equation. *Progr Theoret Phys*. 1997;98:1013–1023.
22. Satsuma J, Ablowitz MJ. Two-dimensional lumps in nonlinear dispersive systems. *J Math Phys*. 1979;20:1496–1503.
23. Ma HC, Deng AP. lump solution of (2+1)-dimensional Boussinesq equation. *Commun Theor Phys*. 2016;65:546–552.
24. Yang JY, Ma WX. Lump solutions to the BKP equation by symbolic computation. *Int J Mod Phys B*. 2016;30(1–7), 1640028.
25. Paul GC, Eti F, Kumar D. Dynamical analysis of lump, lump-triangular periodic, predictable rogue and breather wave solutions to the (3+1)-dimensional gKP–Boussinesq equation. *Results Phys*. 2020;19, 103525.
26. Ma WX. Lump-type solutions to the (3+1)-Dimensional Jimbo-Miwa Equation. *Int J Nonlinear Sci Numer Stimul*. 2016;17:355–359.
27. Hossen MB, Roshid HO, Ali MZ. Multi-soliton, breathers, lumps and interaction solution to the (2+1)-dimensional asymmetric Nizhnik- Novikov-Veselov equation. *Heliyon*. 2019;5(10), e02548.
28. Hoque MF, Roshid HO, Alshammari FS. Dynamical interactions between higher-order rogue waves and various forms of n-soliton solutions of the (2+1)-dimensional ANNV equation. *Chinese Phys B*. 2020;29, 114701.
29. Akhmediev N, Ankiewicz A, Taki M. Waves that appear from nowhere and disappear without a trace. *Phys Lett A*. 2009;373:675–678.
30. Kumar S, Mohan B, Kumar R. Lump, soliton, and interaction solutions to a generalized two-mode higher order nonlinear evolution equation in plasma physics. *Nonlinear Dyn*. 2022;110:693–704.
31. Yin YH, Lu X, Ma WX. Bäcklund transformation, exact solutions and diverse interaction phenomena to a (3+1)-dimensional nonlinear evolution equation. *Nonlinear Dyn*. 2022;108:4181–4194.
32. Yao SW, Nuruzzaman M, Kumar D, Tamanna N, Inc M. Lump solutions to an integrable (3 + 1)-dimensional Boussinesq equation and its dimensionally reduced equations in shallow water. *Results Phys*. 2023;45, 106226.
33. Zhang LL, Lü X, Zhu SZ. Painlevé analysis, Bäcklund transformation and soliton solutions of the (2+1)-dimensional variable-coefficient Boussinesq Equation. *Int J Theor Phys*. 2024;63:160.
34. Kumar S, Rani S. Study of exact analytical solutions and various wave profiles of a new extended (2+1)-dimensional Boussinesq equation using symmetry analysis. *J Ocean Eng Sci*. 2022;7(5):475–484.
35. Sulaiman TA, et al. Wave solutions to the more general (2+1)-dimensional Boussinesq equation arising in ocean engineering. *Int J Mod Phys B*. 2023;37(22), 2350214.
36. Liu JG, Zhu WH. Multiple rogue wave solutions for (2+1)-dimensional Boussinesq equation. *Chin J Phys*. 2020;67:492–500.
37. Kaur L, Wazwaz AM. Dynamical analysis of lump solutions for (3+1) dimensional generalized KP–Boussinesq equation and its dimensionally reduced equations. *Phys Scr*. 2018;93(7), 075203.
38. Singh S, et al. Dynamics of higher order bright and dark rogue waves in a new (2+1)-Dimensional Integrable Boussinesq model. *Phys Scr*. 2020;95(11), 115213.
39. Lü X, Wang JP, Lin FH, Zhou XW. Lump dynamics of a generalized two-dimensional Boussinesq equation in shallow water. *Nonlinear Dyn*. 2018;91(2):1249–1259.
40. Wang XB, et al. On integrability and quasi-periodic wave solutions to a (3+1)-dimensional generalized KdV-like model equation. *Appl Math Comput*. 2016;283: 216–233.
41. Wang XB, Tian SF, Feng LL, Yan H, Zhang TT. Quasiperiodic waves, solitary waves and asymptotic properties for a generalized (3 + 1)-dimensional variable coefficient B-type Kadomtsev–Petviashvili equation. *Nonlinear Dyn*. 2017;88:2265–2279.
42. Hirota R. Exact solutions of the Korteweg–de Vries equation for multiple collisions of solitons. *Phys Rev Lett*. 1971;27(18):1192–1194.